Nordic Hydrology, 21, 1990, 341-354

Changes in the Flexural Strength of Ice under Radiation Decay

Paper presented at the 8th Northern Res. Basins Symposium/Workshop
(Abisko, Sweden – March 1990)

T. D. Prowse, M. N. Demuth and H. A. M. Chew
Environment Canada, Saskatoon, Sask. S7N 3H5, Canada

The strength of an ice cover significantly affects the timing and severity of breakup on northern rivers. During the pre-breakup period, thermal and radiative warming is known to significantly decrease such strength. Although reductions in strength with temperature are reasonably well known, there is a dearth of data concerning strength changes due to internal radiative melt. In the spring of 1989, near Floral, Saskatchewan, Canada, a detailed series of experiments were conducted to determine changes in flexural strength, porosity and optical properties of the ice cover. The test data strongly support existing theoretical models of strength reduction due to porosity development in columnar grained ice. Experimental methods and results with respect to flexural testing, porosity determinations and radiation energy balance are discussed.

Introduction

Spring runoff, often the major flow event of the year, occurs in most cold, northern regions while the main flow channels are ice-covered. Although some reasonably reliable methods exist for measuring flow beneath stable ice covers, little is known about flow conditions during the period of ice breakup. It is often during breakup that peak spring flow is attained and, because of the additional flow resistance created by rough and frequently thick masses of fragmented ice, peak water levels due to backwater effects are also reached. Due to complex interactions between hydrodynamic and thermodynamic processes, our ability to predict the timing,

magnitude and severity of breakup conditions, and to model the downstream progression of the flood wave, is poor. Hence, this is the period of the year, during which our knowledge of flow conditions on northern rivers is the weakest. Unfortunately, this is also the period of peak annual discharge in many northern hydrologic regions. To improve the capability to model breakup flow conditions, increased knowledge about the transient flow system associated with breakup surges and the resistance to breakup offered by the *in-situ* ice cover are required.

Resistance to upstream flow by an ice cover is largely a function of its degree of attachment to the bed and banks, thickness, and competence or mechanical strength, all three of which can decrease during the pre-breakup period. Changes in ice strength are the least understood, but are known to be related to the absorption of solar radiation which results in the development of melt pores within the ice matrix and a reduction in inter-granular contact. Although some attempts have been made to model this process based on theoretical melt geometry, insufficient field data are available for verification. This paper presents a detailed set of field experiments, specifically designed to obtain data concerning changes in flexural strength of an ice cover under radiation decay.

Background Theory

Radiation Balance and Porosity

Absorption of short-wave radiation by an ice cover is known to promote a structural weakening of the ice cover through the development of meltwater pores within the ice matrix. The amount of radiation received by an ice cover during the pre-breakup period depends on the available short-wave radiation, the degree of reflective insulation provided by surface snow and ice, and the timing of breakup. During the early stages of melt, radiation input is consumed largely by surface melt and warming of the ice cover. Significant internal melt does not occur until the ice has reached 0° C, usually after the surface snow has ablated. For snow-free ice, the ice-cover radiation balance is described by

$$R_a = R_i(1-\alpha) - R_H = R_0 - R_H \qquad (1)$$

where R_a is the amount of short-wave radiation absorbed within the ice sheet, R_i and R_o represent the total incoming short-wave radiation before and after losses due to surface reflection, α is the albedo and R_H is the short-wave radiative flux out of the ice bottom at total ice thickness H. Since radiation attenuation within ice is spectrally selective, the spectral composition of R_H can vary considerably from R_i depending on ice thickness and structure. Due to the spectral selectivity of ice and the normal spectral distribution of solar energy, the spectrum from approximately 400 to 850 nm forms the majority of radiation absorbed within relatively thin ice sheets.

Radiation absorption within an ice sheet occurs preferentially at grain boundaries because of a concentration of impurities deposited as part of the freeze-out process. If the rate of heat removal by internal conduction is less than the rate of internal warming from radiation attenuation, localised melt will occur forming melt pores. Once an ice cover reaches a 0° C isothermal condition, all radiative energy is used to produce internal melt. Grain geometry controls the pore arrangement within the ice matrix and, hence, the reduction in grain contact area.

For an isothermal 0° C ice sheet, the melt fraction or porosity (ϕ_l) produced by internal radiative melt is calculated by integration of

$$\frac{d\phi_l}{dt} = \frac{R_a}{\rho_i \lambda_i} \tag{2}$$

where t is time, ϱ_i is the density of ice and λ_i is the latent heat of fusion for ice.

Ice Strength

During the pre-breakup period an ice sheet experiences reductions in strength as it begins to warm to 0° C and subsequently from porosity development. Prowse *et al.* (1991) have shown the latter to be at least as significant as the reduction in confined-compressive strength due to warming from approximately −5° C. Final breakup of an ice cover usually depends on the flexural properties of the ice and involves brittle-elastic fracture.

One of the most common methods for testing the flexural strength of ice is the simply-supported beam test (*e.g.* Schwarz *et al.* 1981). This study employed a 3-point test configuration and elastic theory in which the flexural strength (S_f) can be determined from

$$S_f = 3 P_f \frac{L}{2} W H^2 \tag{3}$$

where P_f is the load at failure, L is the support span length and, W and H are the beam width and thickness, respectively. Because the effects of buoyancy are negligible for the size of beam tested, subgrade reaction influences are not considered in this analysis. Futhermore, vertical variation in ice properties have been ignored, although those related to temperature differences should be small, since the experimentation focussed primarily on isothermal conditions.

Porosity-Strength Relationships

Although the strength of thawing ice has been the focus of a number of research experiments (Bulatov 1970; Frankenstein 1961), establishing a relationship between strength and porosity has been hampered by the lack of concurrent measurements of the radiation balance and thermal condition of the ice cover. Using simplified grain geometries, Bulatov (1970) and Ashton (1985) developed theoretical curves which form a lower envelope to the broad scatter of the then available data. Subsequently, Prowse *et al.* (1988) presented data for columnar grained river

ice (based on "borehole jack" tests), which closely tracked the predicted theoretical decrease of relative strength. Despite the corroborative data obtained by Prowse *et al.* (1988), additional information is required to properly define the porosity-strength relationships for various river ice types and loading conditions. This is especially important for low porosities since the theoretical relationships indicate that this is where the most rapid changes in ice strength occur.

The effect of pore space on sea-ice strength has also been addressed (see review by Weeks and Ackley 1982). Strength reductions were modelled as a function of brine volume and the associated reduction in contact area expressed as

$$\frac{S}{S_0} \cong \frac{A}{A_0} \tag{4}$$

where S is the effective strength, S_0 is the homogeneous (no brine volume) strength and, correspondingly, A represents the effective contact area and A_0 the homogeneous area. This substructure-based approach, coupled with an assumed void geometry led to a relationship of the form

$$\frac{S}{S_0} = 1 - c(\phi_1)^k \tag{5}$$

where c and k are constants defining the strength reduction, the latter term determined by void geometry. As cautioned by Mellor (1983), the use of such relationships can only be considered reasonable if the distribution of porosity with respect to principle stresses does not vary. Given the vertically-regressive, porous structure produced by radiation decay of columnar, fresh-water ice, Ashton's (1985) model can be considered to be a reasonable application of the substructure approach. The values of k and c for this model are 0.5 and 2.813 respectively.

Study Site, Instrumentation and Methodology

Study Site

Field tests were conducted at "Floral Pond", a 35 ha body of water located 8 km east of Saskatoon, Canada. Low snowfall in this region and windswept winter conditions ensure a cover comprised predominantly of columnar grained ice. Owing to the continental climate of the region, clear-sky high-radiation conditions typically characterize the melt period.

A 20 by 30 m-zone was cordoned off on the pond ice surface for field experiments during the 1989 spring season. Mean water depth in this zone was approximately 5 m, with a maximum pre-breakup ice thickness of approximately 0.8 m.

Instrumentation

Thermal and Radiation Balance – At the centre point of one end of the study site, a meteorologic station was established to measure radiation, sunshine hours, air

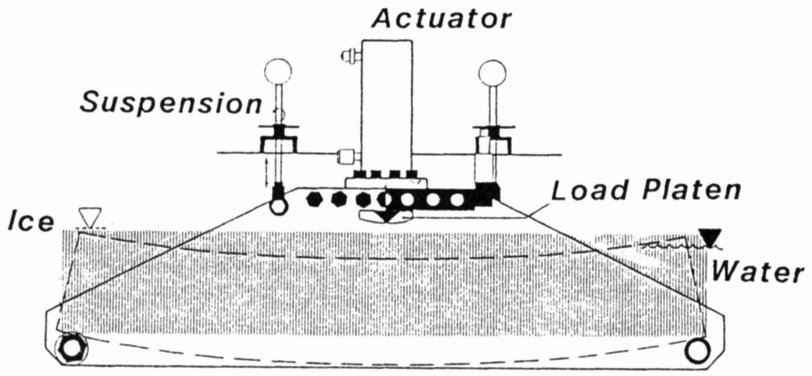

Fig. 1. Schematic of test frame and field installation. Flexural failure precipitated at bottom of ice samples.

temperature, windspeed and humidity. A vertical array of thermistors was also frozen into the cover and shielded from local radiative warming to obtain ice and water temperatures at 0.1 m intervals.

The radiation balance system consisted of silicon photodiodic detectors for measuring photosynthetically active radiation (PAR) over the wave band from 400 to 700 nm (response time of 10 μs). Two surface sensors with a sensitivity af 8 μA

per 1,000 μMol s^{-1} m^{-2} measured incoming and reflected radiation at a height of 1 m above the ice surface. An additional underwater sensor with a sensitivity of 3 μA per 1,000 μMol s^{-1} m^{-2} measured radiation penetrating the ice cover. An underwater, floating housing was used to orient the sensor directly beneath and level with the ice cover bottom.

Ice Flexural Strength – Flexural strength measurements were obtained using a hydraulic reaction frame (Demuth and Prowse 1989) which permitted *in-situ* testing of ice beams sawn from the parent ice sheet (Fig. 1). The frame was designed so that reaction forces resulting from the beam test were transferred to the frame rather than the surrounding ice sheet thus achieving maximum test system stiffness. *In-situ* testing is particularly important for the testing of "warm" (near 0° C) ice because it precludes any unnatural modification of the thermodynamic regime that might otherwise occur if the ice was extracted for surface testing.

To ensure that the bending experiments precipitated a brittle-elastic fracture, a load compensated flow control was used to maintain a sufficient constant rate of deflection. Load and deflection changes were recorded as a function of time. Nominal stress-rate for all tests was approximately 3.5 MPa s^{-1}. Measurements of beam dimensions and basic ice structure were obtained for each specimen. Tests were conducted over approximately the same time interval each day. Beam support span (L) ranged from 1.5-2.5 m.

Results

Hydrometeorologic Conditions

Because of warm and sunny conditions near the end of March (Fig. 2), most snow had ablated by April 1. The thermal regime of the main body of the ice sheet reached an isothermal 0° C condition by April 3, except near the surface where nocturnal cooling reduced temperatures to below 0° C over the night and early morning hours. This latter effect is believed to have had a negligible effect on the porosity or strength because: a) it affected only the uppermost ice strata (<0.1 m) and, b) the surface was observed to have returned to a melting state each day before the main input of radiation occurred and before strength testing resumed. The only significant cold period occurred on April 7-8 when approximately 20 mm of snow fell and negative maximum air temperatures were briefly recorded. By April 9, warm conditions had returned and the snowcover was completely ablated. Radiation receipts were appreciably reduced over this two-day period, although the magnitude and brevity of the event did not produce significant refreezing of the ice cover. Over the strength-testing period, ice cover thickness decreased from 0.76 m on March 23 to 0.48 m on April 13.

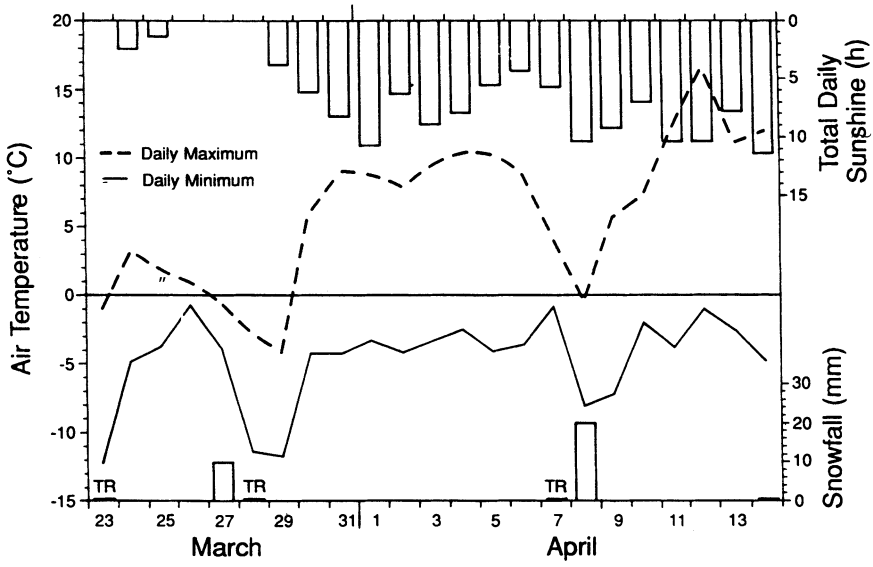

Fig. 2. Meteorologic conditions during the period of ice testing, 1989.

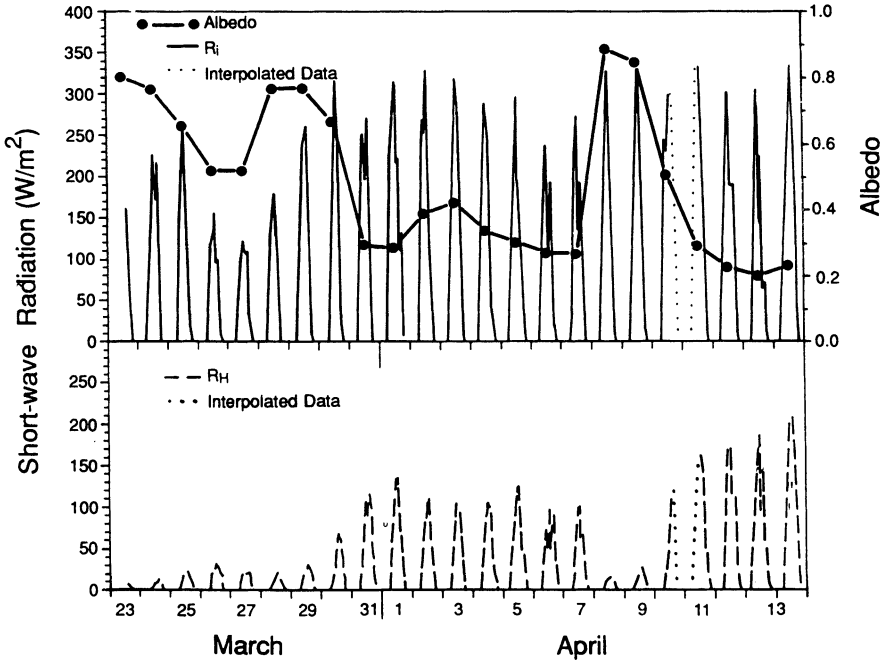

Fig. 3. Incident shortwave radiation, surface albedo, and radiation at ice base (400-700 nm).

Radiation Receipts and Porosity Development

Measurements of incoming radiation, radiation received at the ice base and albedo are shown in Fig. 3. After the ice became isothermal, daily peak values of R_i ranged from approximately 250-350 W m^{-2} and albedo values for the snow-free surface were in the range 0.2-0.4 except for a brief rise associated with the April 7-8 snowfall. During this two day period, R_H values dropped below 30 W m^{-2} but under snow-free conditions were generally in the 100-200 W m^{-2} range.

Since available equipment only permitted the direct measurement of PAR, calculated values of R_a from Eq. (1) had to be increased to account for the entire 400-850 nm melt spectrum. This was accomplished by a) normalizing a spectral irradiance curve obtained from Grenfell and Perovich (1984) at 50 nm bandwidths over the 400-850 nm range, b) inserting these values with extinction coefficients for melting blue ice (Grenfell and Maykut 1977), and average-daily ice thicknesses obtained from the test results, in

$$R_{a,m} = R_{o,m}(1-e^{-\kappa,m H}) \tag{6}$$

where m refers to a specific bandwidth, κ is the extinction coefficient and H is ice thickness. c) calculating the ratio of absorbed radiation between the two bandwidths from 400 to 700 nm ($R_{a,\Sigma 400\text{-}700}$) and 400 to 850 nm ($R_{a,\Sigma 400\text{-}850}$), ϵ

$$\epsilon = \frac{R_{a,\Sigma 400-850}}{R_{a,\Sigma 400-700}} \tag{7}$$

and d) using this ratio to obtain the total radiative flux

$$R_a = \epsilon R_{a,\Sigma 400-700} \tag{8}$$

These final R_a values were then used in Eq. (2) to obtain daily values of porosity as shown in Fig. 4. The effects of spectral filtering on R_o through reflective losses were not considered in this approach, but are believed to be small for ice sheets comprised of large-grained columnar ice.

Flexural Properties

Flexural testing at Floral Pond began on March 23 and ended on April 15. A total of 90 beam tests were performed, 50 after the ice sheet had attained a 0° C isothermal condition (April 3). By April 9, the ice cover was too weak to permit the mechanical extraction of intact beams for use in the reaction frame. Further tests were conducted using manually deflected (upward) cantilever beams for which the flexural strength (S_{fc}) is given by

$$S_{fc} = 6 P_f \frac{L}{W} H^2 \tag{9}$$

As noted by Lavrov (1971), cantilever test results can be related to those obtained

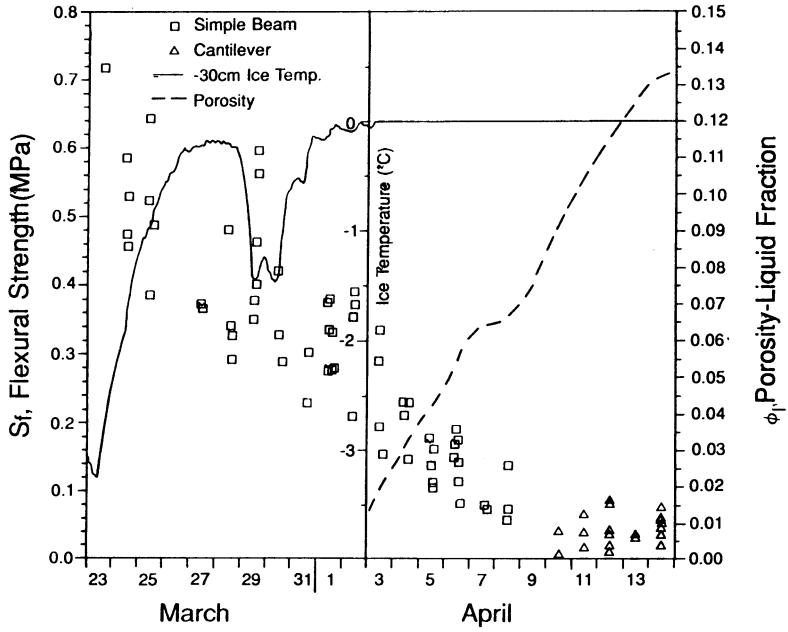

Fig. 4. Flexural strength, ice temperature and porosity.

using 3-point simple support techniques by

$$S_f = 1.5\, S_{fc} \tag{10}$$

Fig. 4 illustrates the deterioration of flexural strength throughout the study period. Initial beam tests conducted on March 23-24, with mid-thickness ice temperatures at approximately −2.5° C, resulted in a mean value for S_f of 0.55 MPa (standard deviation of ±0.11). Strength subsequently decreased as the ice sheet warmed until a cooling/snowfall event on March 29 resulted in a temporary increase in flexural strength. Further warming produced a 0° C isothermal state on April 3, with S_f having reduced to a mean value of 0.32 MPa (standard deviation ±0.06).

Significant diurnal variations in strength were not observed, largely because tests were conducted with the bottom surface in tension. Bending failure is normally characterized by crack initiation at the tensile surface, but the bottom ice strata was effectively insulated from the diurnal changes in thermal regime. To assess differences in upward versus downward flexural strength, a few tests were also conducted with the top surface in tension (ϕ_l = 0.05 to 0.07) but these revealed no significant differences in flexural strength. Sample time, however, did not permit testing over the full range of porosities nor over a full diurnal period.

With a gradual increase in porosity to approximately 0.09 on April 9, mean S_f gradually decreased to only 0.04 MPa. Subsequent cantilever test results found S_f to remain approximately constant for $\phi_l > 0.09$.

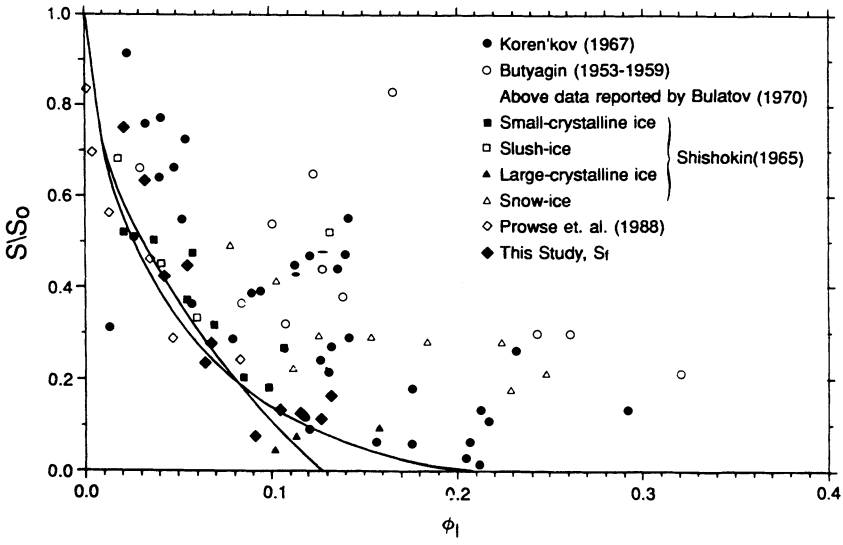

Fig. 5. Available data regarding strength-porosity relationship.

Analysis and Discussion

Data in Fig. 4 indicate that the magnitude of deterioration during radiation decay is larger than that produced by warming from −2.5° C to 0° C. Specifically, S_f declined by 0.23 MPa (42 %) during the warming period, in contrast to the 0.28 MPa (88 %) decrease associated with the increase in porosity to ≈0.09. Furthermore, it appears from Fig. 4 that porosities greater than approximately 0.1 do not have a measurable effect on ice strength. Data reviewed by Weeks and Assur (1972) concerning sea ice, also indicate that flexural strength is not significantly modified by brine volume (porosity) beyond 0.1. Notably, a porosity of 0.1 has been suggested by Prowse *et al.* (1989) to be an upper limit with respect to the initiation of river ice breakup.

To permit comparison of the flexural data with other strenght data, a simple non-dimensional ratio, (S/S_o), is used. S_f data are normalized using the homogeneous undecayed strength of S_{fo} = 0.32 MPa and plotted against porosity (Fig. 5). These data provide good corroboration of the theoretical curves proposed by Bulatov (1970) and Ashton (1985) over the entire range of expected porosities. For further comparison, it is useful to plot the data showing significant strength changes (*i.e.*, ϕ_l = 0.00-0.09) according to the melt-geometry approach of Eq. (5). Hence

$$\frac{S_f}{S_{fo}} = 1 - 2.717(\phi_l)^{\frac{1}{2}} \qquad (11)$$

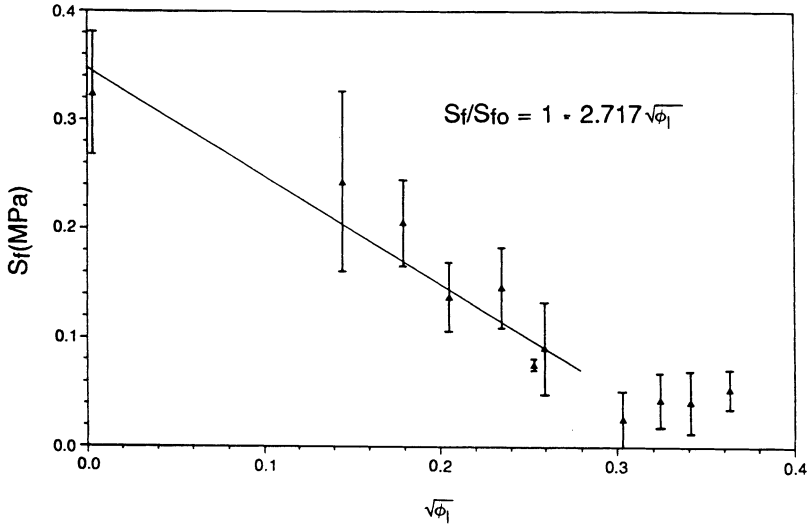

Fig. 6. Flexural strength versus porosity, this study. Bars indicate standard deviation about mean values.

with $R^2 \equiv 0.93$ (Fig. 6). c is in good agreement with the 2.813 value derived by Ashton (1985) for the theoretical relationship.

While the data from this report supports the general shape of the theoretical curves in Fig. 5, particularly that of Ashton (1985); it is important to note that they were obtained from large ice samples comprised of grain-pore geometries significantly more complex than those assumed by the theoretical models. Furthermore, the analysis employed a bulk porosity, whereas porosity probably varied substantially in the vertical. The effect of such variations on the flexural strength of large samples must be addressed in further experiments.

From the theoretical modelling perspective, further refinement must be made about the assumed melt geometry and related changes in strength due to reductions in contact area. For example, Prowse *et al.* (1989) observed that laboratory-grown columnar ice showed evidence of uniform surface melt along grain facets and not a concentration of melt at intergranular contact points as assumed by both theoretical models. The role of pore size, shape and distribution should also be assessed in reference to changes in strength. In particular, some attention should focus on Bulatov's (1970) proposed "kinetic attachment" of melting grains; a process produced by internal friction forces and varying according to the rate of grain detachment.

Conclusions

The relationship between porosity and flexural strength of columnar ice established in this paper provides some verification of the functions generated by the theoretical models of Bulatov (1970) and Ashton (1985). Questions remain, however, regarding the actual melt geometry produced by radiation absorption and the associated reduction in strength. Specifically the role and relative importance of contact-area and attachment forces between ice and water must be evaluated. This is particularly important at the initial stages of porosity development since this is where the most rapid decrease in strength occurs.

Future work should also be oriented towards incorporating the porosity-strength relationship into forecast models of river ice breakup. The polymorphic nature of river ice covers, requires the ability to account for composite ice sheet structures. Therefore, strength-energy balance relationships will have to be established for other ice types, especially for polycrystalline ice which often characterizes the surface of river ice covers – the zone of greatest radiation input. Furthermore, to provide further verification of these test results and to ensure that data from localized mechanical testing can be used in full-scale analyses, the analytical methodology should be extended to account for vertical profile varitions in porosity and its influence on flexural behaviour.

Acknowledgements

The authors thank Messrs. C. Onclin, R. MacKay, N. Hedstrom, B. McCarthy and other technical staff of the National Hydrology Research Institute (NHRI) for their valuable assistance in the field and data analysis, Mr. T. Maxin (NHRI) for electronic equipment assembly, and Drs. R. Frederking and G. Timco (National Research Council of Canada) for useful comments made during the initial planning stages of ice testing. The authors are also indebted to Mr. E. Brown, for his assistance in the storage of field equipment and Mr. J. Agar for access to the study site.

List of Symbols

A	– effective contact area (m^2)
A_o	– homogeneous (undecayed) contact area (m^2)
H	– ice and beam thickness (m)
L	– support span length (m)
P_f	– load at failure (MN)
R_a	– total absorbed short-wave radiation ($W\ m^{-2}$)
R_H	– total outgoing short-wave radiation (at ice bottom) ($W\ m^{-2}$)

R_i - total incoming short-wave radiation (W m^{-2})
R_o - total incoming short-wave radiation after reflective loss (W m^{-2})
S - strength (general) (MPa)
S_f - flexural strength (MPa)
S_{fc} - flexural strength as derived by cantilever beam test (MPa)
S_{fo} - undecayed 0° C flexural strength (MPa)
S_o - undecayed 0° C strength (MPa)
W - beam width (m)
c - constant in Eq. (5)
k - constant in Eq. (5)
m - subscript: bandwidth
t - time (s)
α - albedo
ϵ - ratio of radiative fluxes
κ - extinction coefficient (m^{-1})
ϱ_i - ice density (kg m^{-3})
λ_i - latent heat of fusion of ice (J kg^{-1})
ϕ_l - porosity-liquid fraction
Σ400-700 - subscript corresponding to 400-700 nm bandwidth
Σ400-850 - subscript corresponding to 400-850 nm bandwidth

References

Ashton, G. D. (1985) Deterioration of floating ice covers, *J. Energy Resour. Technol., Vol. 107,* pp. 177-182.

Bulatov, S. N. (1970) Calculating the strength of thawing ice cover and the beginning of wind activated drift, Trudy Vypysk, 74, Gidrometeorologisheskoye Izdatel'stvo, Leningrad. Translation by US Army CRREL, IR 799, 120 pp.

Demuth M. N., and Prowse, T. D. (1989) A hydraulically actuated test frame for the field determination of ice flexural properties, Proc. 46th Annual Eastern Snow Conference, Quebec City, Canada, pp. 242-246.

Frankenstein, G. E. (1961) Strength data on lake ice, US Army SIPRE Technical Report 80, 18 pp.

Grenfell, T. C., and Maykut, G. A. (1977) The optical properties of ice and snow in the Arctic Basin, *J. Glaciol., Vol. 22* (87), pp. 305-320.

Grenfell, T. C., and Perovich, D. K. (1984) Spectral albedos of sea ice and incident solar irradiance in the Southern Beaufort Sea, *J. Geophys. Res., Vol. 76(6),* pp. 1550-1575.

Lavrov, V. V. (1971) Deformation and strength of ice, National Science Foundation Translation-Israel Program for Scientific Translation, Jerusalem, 64 pp.

Mellor, M. (1983) Mechanical behaviour of sea ice, US Army CCREL Monograph 83-1, 105 pp.

Prowse, T. D., Demuth, M. N., and Onclin, C. R. (1988) Using the borehole jack to determine changes in river ice strength, Proc. 5th Workshop on the Hydraulics of River Ice/Ice Jams, 1988, Winnipeg, Canada, pp. 283-301.

Prowse, T. D., Demuth, M. N., and Chew, C. R. (1989) The strength and radiation-induced decay of river ice: A review of processes, theories and current NHRI research, Environment Canada, National Hydrology Research Institute, Report CS-89053, 27 pp.

Prowse, T. D., Demuth, M. N., and Chew, C. R. (1991) The deterioration of freshwater ice due to radiation decay, *J. Hydraul. Res.* (in press).

Schwarz, J., Frederking, R., Gavrillo, V., Petrov, I. G., Hirayama, K. I., Mellor, M., Tryde, P., and Vaudrey, K. D. (1981) Standardized testing methods for measuring mechanical properties of ice, *Cold Reg. Sci. Technol., Vol. 4,* pp. 245-253.

Weeks, W. F., and Ackely, S. F. (1982) The growth, structure and porosity of sea ice. US Army CRREL Monograph 82-1, 130 pp.

Weeks, W. F., and Assur, A. (1972) Fracture of lake and sea ice. In: *Fracture, An Advanced Treatise;* H. Liebowitza, ed., Vol. 7, Fracture of Nonmetals and Composites, Academic Press, pp. 879-978.

First received: 27 February, 1990
Accepted: 28 May, 1990

Address:
National Hydrology Research Institute,
Environment Canada,
Saskatoon, Sask. S7N 3H5,
Canada.